

## Rapid Structural Identification of Cytotoxic Bufadienolide Sulfates in Toad Venom from *Bufo melanostictus* by LC-DAD-MS<sup>n</sup> and LC-SPE-NMR

Huimin Gao,<sup>†</sup> Martin Zehl,<sup>‡</sup> Hanspeter Kaehlig,<sup>§</sup> Peter Schneider,<sup>⊥</sup> Hermann Stuppner,<sup>⊥</sup> Laetitia Moreno Y. Banuls,<sup>||</sup> Robert Kiss,<sup>||</sup> and Brigitte Kopp<sup>\*,‡</sup>

Institute of Chinese Materia Medica, China Academy of Chinese Medical Sciences, Beijing 100700, People's Republic of China, Department of Pharmacognosy, University of Vienna, A-1090 Vienna, Austria, Institute of Organic Chemistry, University of Vienna, A-1090 Vienna, Austria, Institute of Pharmacy/Pharmacognosy, University of Innsbruck, A-6020 Innsbruck, Austria, and Laboratory of Toxicology, Institute of Pharmacy, Université Libre de Bruxelles, 1050 Brussels, Belgium

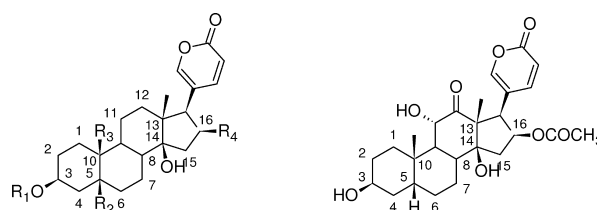
Received November 17, 2009

Toad venom, namely, “Chansu” in China, has been widely used for the treatment of heart failure, sores, pains, and various cancers. Upon LC-MS analysis of the venom from *Bufo melanostictus* collected in Indonesia, new bufadienolide sulfates were identified. For a complete characterization, the MeOH extract of the toad venom from *B. melanostictus* was fractionated by preparative HPLC, and the structures of five new bufadienolide sulfates (**1–5**) along with one new bufogenin (**6**) were rapidly elucidated on the basis of LC-DAD-MS<sup>n</sup> and LC-SPE-NMR data. The in vitro growth inhibitory activity of these six compounds along with hellebrin (positive control) has been assayed by means of the MTT colorimetric assay in four human and two mouse cancer cell lines. Compound **3** and hellebrin displayed similar and marked in vitro cytotoxicity.

Toad venom, namely, “Chansu” in China, has been widely used to treat heart failure, sores, and pains, and, recently, for the treatment of various cancers. According to the current Chinese Pharmacopoeia, the dried secretion of two different *Bufo* species, *B. bufo gargarizans* Cantor and *B. melanostictus* Schneider, is recorded as toad venom.<sup>1</sup> *B. melanostictus* was thus investigated in several chemical and pharmacological studies. A number of diverse compounds such as sterols,<sup>2</sup> bufogenins,<sup>3,4</sup> and bufotoxins<sup>5</sup> have been isolated from its venom and skin. The comprehensive pharmacological evaluation indicated that the skin extracts of this species possessed broad bioactivity, including cardiotoxic, antineoplastic, neurotoxic, immunomodulatory, antimicrobial, and sleep potentiation activity.<sup>6–8</sup> We have detected previously unknown compounds in *B. melanostictus* from Indonesia by preliminary LC-MS analysis. In the present investigation, the structures of six new bufadienolides (**1–6**) were elucidated by LC-DAD-MS<sup>n</sup> and LC-SPE-NMR. The in vitro growth inhibitory activity of these six compounds along with hellebrin (positive control) has been assayed by means of the MTT colorimetric assay in four human and two mouse cancer cell lines. Compound **3** and hellebrin displayed similar and marked in vitro cytotoxic activity. This is particularly relevant since bufadienolides are increasingly recognized as interesting antitumor lead compounds. Considering that preparations of toad venom are actually used in China for the treatment of cancer,<sup>6</sup> but are also known to have potentially lethal side effects on the cardiovascular system,<sup>9</sup> an in-depth knowledge of all relevant bioactive constituents is urgently required to understand the effective and toxic mechanisms.

### Results and Discussion

The MeOH extract of the toad venom collected from *B. melanostictus* was subjected to preparative HPLC to give compounds **1–6**. The HPLC profiles of the crude extract and fractions II–V are shown in Figures 2 and 3, respectively. Peaks **1–6** displayed a



**1** R<sub>1</sub>=SO<sub>3</sub>H, R<sub>2</sub>=OH, R<sub>3</sub>=CH<sub>2</sub>OH, R<sub>4</sub>=H

**2** R<sub>1</sub>=SO<sub>3</sub>H, R<sub>2</sub>=OH, R<sub>3</sub>=CHO, R<sub>4</sub>=H

**3** R<sub>1</sub>=SO<sub>3</sub>H, R<sub>2</sub>=H, R<sub>3</sub>=CH<sub>2</sub>OH, R<sub>4</sub>=H

**4** R<sub>1</sub>=SO<sub>3</sub>H, R<sub>2</sub>=H, R<sub>3</sub>=CH<sub>3</sub>, R<sub>4</sub>=OH

**5** R<sub>1</sub>=SO<sub>3</sub>H, R<sub>2</sub>=OH, R<sub>3</sub>=CH<sub>3</sub>, R<sub>4</sub>=H

**Figure 1.** Structures of bufadienolides from toad venom of *B. melanostictus*.

characteristic maximum absorption band at 292–300 nm in online UV spectra due to the  $\alpha$ -pyrone ring at C-17 of bufadienolides.

Compound **1** showed  $\lambda_{\text{max}}$  at 299 nm in the online UV spectrum, which is in accordance with that of hellebrigenol.<sup>4</sup> The molecular weight of **1** was deduced as 498 from the protonated and deprotonated molecular ions at  $m/z$  499 ( $[M + H]^+$ ) and  $m/z$  497 ( $[M - H]^-$ ) detected in positive and negative ion mode LC-ESIMS, respectively. A prominent neutral loss of 80 Da, corresponding to the loss of SO<sub>3</sub>, was observed in positive ion mode MS<sup>1</sup> and MS<sup>2</sup> (Supporting Information, S1). In MS<sup>1</sup>, where typically intact pseudomolecular ions are recorded, this fragmentation occurs unintentionally by activation of the rather labile  $[M + H]^+$  ion in the ion source (i.e., in-source decay), whereas in MS<sup>2</sup> the fragmentation is induced by isolation and subsequent collision-induced dissociation of the selected  $[M + H]^+$  ion in the ion trap. The MS<sup>3</sup> spectrum (i.e., the mass spectrum resulting from further isolation and collision-induced dissociation of a first-generation product ion) of the  $[M - SO_3 + H]^+$  ion at  $m/z$  419 shows identical fragment ions to the reference compound hellebrigenol, including the characteristic neutral loss of 30 Da (CH<sub>2</sub>O) due to the elimination of the hydroxymethyl side chain<sup>10</sup> (Table 1). The <sup>1</sup>H NMR spectrum (S2) of **1** exhibits an ABX-type spin system comprising three aromatic protons at  $\delta$  7.86 (1H, dd,  $J = 9.8, 2.6$

\* Corresponding author. Tel: +43(1)4277-55255. Fax: +43(1)4277-55256. E-mail: brigitte.kopp@univie.ac.at.

<sup>†</sup> Institute of Chinese Materia Medica.

<sup>‡</sup> Department of Pharmacognosy, University of Vienna.

<sup>§</sup> Institute of Organic Chemistry, University of Vienna.

<sup>⊥</sup> University of Innsbruck.

<sup>||</sup> Université Libre de Bruxelles.

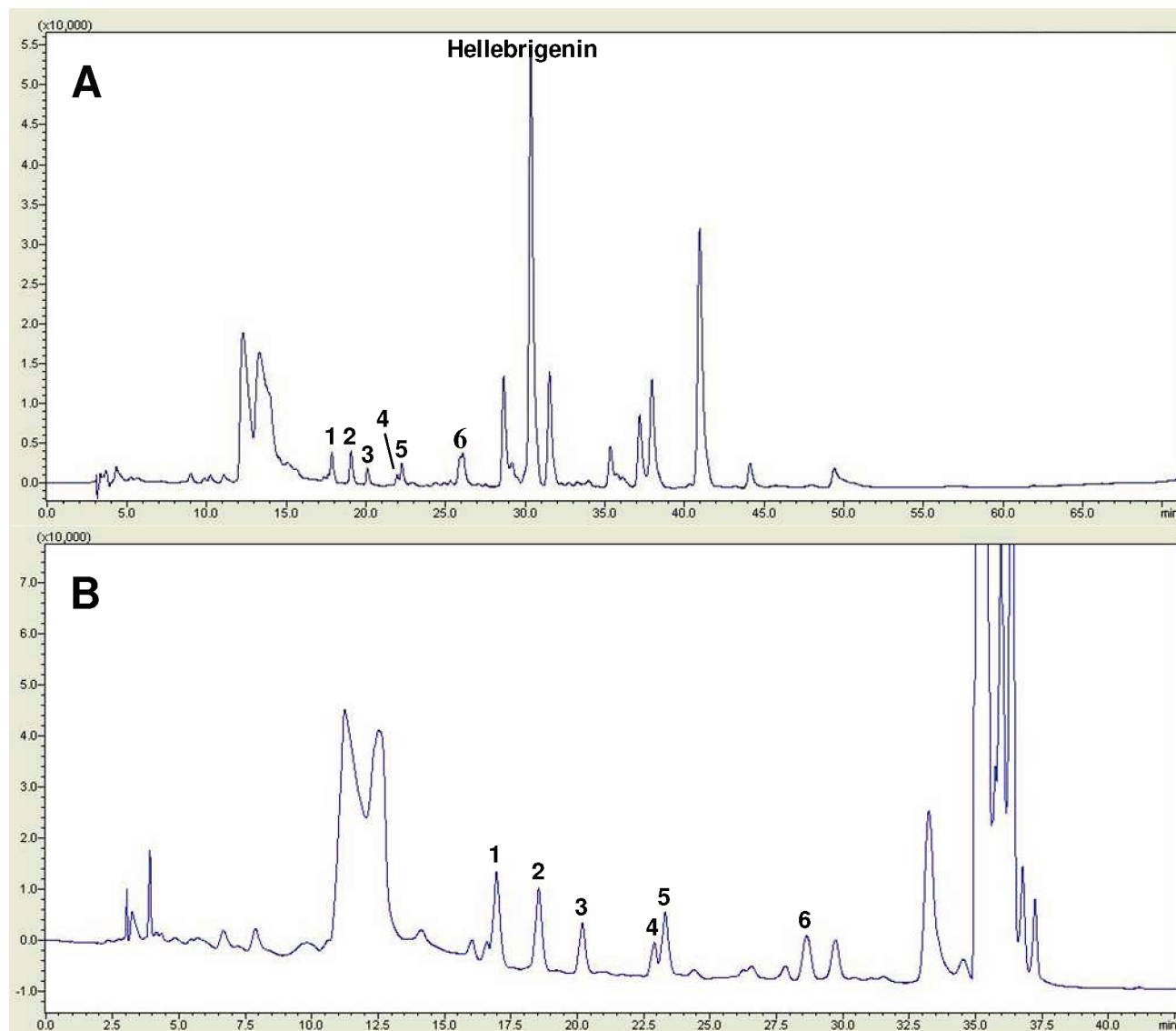


**Figure 2.** HPLC profiles of the MeOH extract of toad venom from *B. melanostictus* at 296 nm. (A) Chromatogram obtained using the mobile phase gradient for analytical HPLC of the crude extract (MeCN, 0–45 min, 8%–54%, 45–55 min, 54%, 55–70 min, 54%–95%). (B) Chromatogram obtained using the optimized mobile phase gradient for preparative HPLC of the crude extract (MeCN, 0–30 min, 15%–28%, 30–31 min, 28%–100%, 31–41 min, 100%).

Hz), 7.29 (1H, d,  $J = 2.6$  Hz), and 6.18 (1H, d,  $J = 9.8$  Hz), which were assigned as H-22, H-21, and H-23 of the  $\alpha$ -pyrone ring. Two additional signals at  $\delta$  4.20 (1H, d,  $J = 11.4$  Hz) and 3.36 (1H, d,  $J = 11.4$  Hz) belong to H-19 $\alpha$  and H-19 $\beta$ . The three-proton singlet at  $\delta$  0.64 indicates the presence of the C-18 methyl group (Table 2). Compared to the  $^{13}\text{C}$  NMR data of hellebrigenol, the resonance of C-3 of **1** is shifted downfield by 8.3 ppm, whereas those of C-2 and C-4 are shifted upfield by 2.4 and 1.2 ppm, respectively (Table 3). These data revealed that the sulfate group was attached to C-3 of hellebrigenol. Accordingly, compound **1** was identified as hellebrigenol-3-*O*-sulfite.

Compound **2** showed  $\lambda_{\text{max}}$  at 299 nm in the online UV spectrum, which is in accordance with that of hellebrigenin.<sup>4</sup> The molecular weight of **2** is only 2 mass units less than compound **1** according to the  $[\text{M} + \text{H}]^+$  and  $[\text{M} - \text{H}]^-$  ions at  $m/z$  497 and 495, respectively. Again, the MS<sup>2</sup> spectrum (S3) of the  $[\text{M} + \text{H}]^+$  ion of **2** was dominated by the neutral loss of 80 Da ( $\text{SO}_3$ ), also observed in MS<sup>1</sup> with high abundance. The base peak in the MS<sup>3</sup> spectrum of the  $[\text{M} - \text{SO}_3 + \text{H}]^+$  ion ( $m/z$  417) of **2** at  $m/z$  335 was interpreted as  $[\text{M} - \text{SO}_3 - 3\text{H}_2\text{O} - \text{CO} + \text{H}]^+$ , indicating the presence of a C-10 formyl group (Table 1).<sup>10</sup> Although hellebrigenin was not available as a reference compound, it was readily identified

as one of the main components of the MeOH extract of the toad venom collected from *B. melanostictus* (Figure 2, A). The LC-ESIMS<sup>2</sup> spectrum of hellebrigenin was identical to the MS<sup>3</sup> spectrum of the  $[\text{M} - \text{SO}_3 + \text{H}]^+$  ion of **2**. The LC- $^1\text{H}$  NMR spectrum (S4) provided evidence for the presence of a C-19 formyl group according to the proton signal at  $\delta$  10.05 and only one signal for a methyl group at  $\delta$  0.63 ppm (3H, s). In addition, the characteristic features of the  $\alpha$ -pyrone ring were also observed, i.e., the resonances at  $\delta$  7.29 (1H, d,  $J = 2.6$  Hz), 7.86 (1H, dd,  $J = 9.8, 2.6$  Hz), and 6.18 ppm (1H, d,  $J = 9.8$  Hz). In the  $^{13}\text{C}$  NMR spectrum of **2**, the chemical shift of C-3 was observed at  $\delta$  76.7, corresponding to a downfield shift of 8.3 ppm compared to hellebrigenin.<sup>11</sup> Thus the structure of **2** was established as hellebrigenin-3-*O*-sulfite.

Compound **3** showed  $\lambda_{\text{max}}$  at 299 nm in the online UV spectrum and a molecular weight of 482 ( $m/z$  483 for the  $[\text{M} + \text{H}]^+$  and  $m/z$  481 for the  $[\text{M} - \text{H}]^-$ ). Loss of  $\text{SO}_3$  by in-source decay was barely detected in MS<sup>1</sup>, which is attributed to the lack of the C-5 hydroxy group. The  $[\text{M} - \text{SO}_3 + \text{H}]^+$  ion at  $m/z$  403 was, however, the base peak in MS<sup>2</sup>, and further fragmentation of this ion in MS<sup>3</sup> gave, among others, the characteristic loss of  $\text{CH}_2\text{O}$ , indicating the presence of the C-19 hydroxy group (Figure 4, Table 1). Because

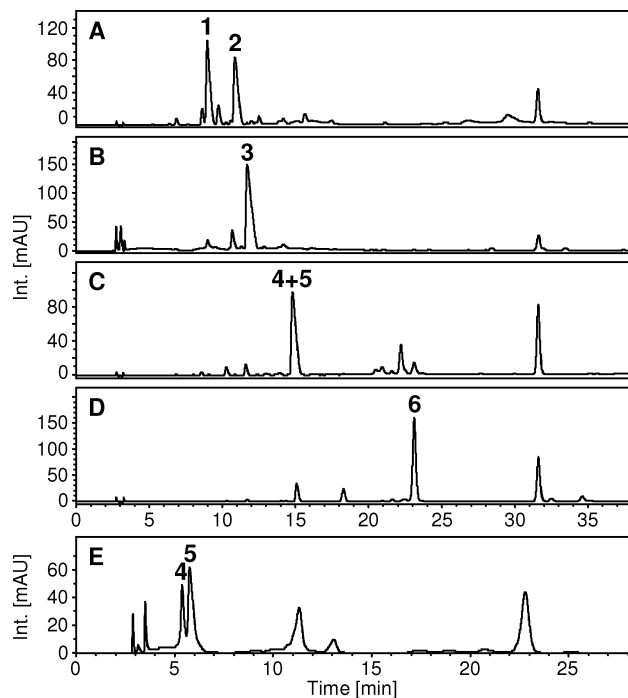


**Figure 3.** HPLC chromatograms (DAD 296 nm) of fractions II–V containing compounds 1–6. Chromatograms A–D, showing fractions II–V, respectively, were obtained on a Hypersil BDS-C<sub>18</sub> column (4.0 × 250 mm, 5 μm). Fraction IV was additionally analyzed on a Nucleosil C<sub>18</sub> column (4.0 × 250 mm, 5 μm) using a shallower gradient to facilitate separation of the isobaric compounds 4 and 5 (E).

**Table 1.** Main Ions of Compounds 1–6 Obtained by HPLC/MS<sup>n</sup>

	UV $\lambda_{\max}$ (nm)	[M + H] <sup>+</sup>	main product ions from [M + H] <sup>+</sup>
1	299	499	419[M - SO <sub>3</sub> + H] <sup>+</sup> , 401[419 - H <sub>2</sub> O] <sup>+</sup> , 383[419 - 2H <sub>2</sub> O] <sup>+</sup> , 371[401 - CH <sub>2</sub> O] <sup>+</sup> , 365[419 - 3H <sub>2</sub> O] <sup>+</sup> , 353[383 - CH <sub>2</sub> O] <sup>+</sup> , 347[419 - 4H <sub>2</sub> O] <sup>+</sup> , 335[365 - CH <sub>2</sub> O] <sup>+</sup> , 317[347 - CH <sub>2</sub> O] <sup>+</sup>
2	299	497	417[M - SO <sub>3</sub> + H] <sup>+</sup> , 399[417 - H <sub>2</sub> O] <sup>+</sup> , 381[417 - 2H <sub>2</sub> O] <sup>+</sup> , 363[417 - 3H <sub>2</sub> O] <sup>+</sup> , 353[381 - CO] <sup>+</sup> , 345[417 - 4H <sub>2</sub> O] <sup>+</sup> , 335[363 - CO] <sup>+</sup> , 317[345 - CO] <sup>+</sup>
3	299	483	403[M - SO <sub>3</sub> + H] <sup>+</sup> , 385[403 - H <sub>2</sub> O] <sup>+</sup> , 367[403 - 2H <sub>2</sub> O] <sup>+</sup> , 349[403 - 3H <sub>2</sub> O] <sup>+</sup> , 337[367 - CH <sub>2</sub> O] <sup>+</sup> , 253[349 - C <sub>5</sub> H <sub>4</sub> O <sub>2</sub> ] <sup>+</sup>
4	296	483	465[M - H <sub>2</sub> O + H] <sup>+</sup> , 447[M - 2H <sub>2</sub> O + H] <sup>+</sup> , 403[M - SO <sub>3</sub> + H] <sup>+</sup> , 385[403 - H <sub>2</sub> O] <sup>+</sup> , 367[403 - 2H <sub>2</sub> O] <sup>+</sup> , 349[403 - 3H <sub>2</sub> O] <sup>+</sup> , 339[367 - CO] <sup>+</sup> , 331[403 - 4H <sub>2</sub> O] <sup>+</sup> , 321[349 - CO] <sup>+</sup> , 307[403 - C <sub>5</sub> H <sub>4</sub> O <sub>2</sub> ] <sup>+</sup> , 303[331 - CO] <sup>+</sup> , 253[349 - C <sub>5</sub> H <sub>4</sub> O <sub>2</sub> ] <sup>+</sup> , 215
5	299	483	403[M - SO <sub>3</sub> + H] <sup>+</sup> , 385[403 - H <sub>2</sub> O] <sup>+</sup> , 367[403 - 2H <sub>2</sub> O] <sup>+</sup> , 349[403 - 3H <sub>2</sub> O] <sup>+</sup>
6	292	475	415[M - HOAc + H] <sup>+</sup> , 397[415 - H <sub>2</sub> O] <sup>+</sup> , 379[415 - 2H <sub>2</sub> O] <sup>+</sup> , 369[397 - CO] <sup>+</sup> , 361[415 - 3H <sub>2</sub> O] <sup>+</sup> , 351[379 - CO] <sup>+</sup> , 333[361 - CO] <sup>+</sup>

of the low amount of isolated fraction III, the quality of the LC-<sup>1</sup>H NMR data was insufficient to unambiguously identify the structure of 3. However, on the basis of the MS<sup>3</sup> spectrum of the [M - SO<sub>3</sub> + H]<sup>+</sup> ion of 3, which is identical to the MS<sup>2</sup> spectrum of the reference compound 19-hydroxybufalin,<sup>4</sup> the structure of 3 may be proposed as 19-hydroxybufalin-3-*O*-sulfite.

Compounds 4 and 5 showed nearly identical retention times on the Hypersil BDS C<sub>18</sub> column and could not be resolved under the same HPLC conditions as employed for compounds 1–3. Better separation was achieved on a Nucleosil C<sub>18</sub> column and elution with a shallower gradient (Figure 3, B). Compounds 4 and 5 were

isobaric, with a molecular weight of 482 ( $m/z$  483 for the [M + H]<sup>+</sup>) but yielded different online UV and ESIMS<sup>n</sup> spectra. Peak 4 showed a hypsochromic shift to give  $\lambda_{\max}$  at 296 nm due to a substituent at C-16, whereas peak 5 showed  $\lambda_{\max}$  at 299 nm. Compound 4 yielded a neutral loss of SO<sub>3</sub> upon MS<sup>2</sup> of the [M + H]<sup>+</sup> ion, but showed very little in-source decay, which is again attributed to the lack of the C-5 hydroxy group (S5). The most abundant product ions in MS<sup>2</sup> of 4 were assigned as [M - SO<sub>3</sub> - 2H<sub>2</sub>O + H]<sup>+</sup> at  $m/z$  367 and [M - SO<sub>3</sub> - 3H<sub>2</sub>O + H]<sup>+</sup> at  $m/z$  349. Fragment ions of the same mass (i.e., [M - 2H<sub>2</sub>O + H]<sup>+</sup> at  $m/z$  367 and [M - 3H<sub>2</sub>O + H]<sup>+</sup> at  $m/z$  349) were observed in the MS<sup>2</sup> spectrum of the [M + H]<sup>+</sup> ion of the reference compound desacetylbufotalin.<sup>4</sup> The MS<sup>3</sup> spectra of the two corresponding ions at  $m/z$  367 of 4 and desacetylbufotalin were similar, suggesting that 4 could be the desacetylbufotalin-3-*O*-sulfite. Compound 5, on the contrary, exhibited significant neutral loss of SO<sub>3</sub> due to in-source decay. The relative abundance of the [M - SO<sub>3</sub> + H]<sup>+</sup> ion was in fact so high in MS<sup>1</sup> that the data-dependent acquisition yielded only pseudo-MS<sup>3</sup> spectra of this in-source fragment ion instead of MS<sup>2</sup> spectra of the intact [M + H]<sup>+</sup> ion (S6). The pseudo-MS<sup>3</sup> spectrum of the [M - SO<sub>3</sub> + H]<sup>+</sup> ion of compound 5, which mainly shows successive neutral loss of three molecules of water, is identical with the MS<sup>2</sup> spectrum of the [M + H]<sup>+</sup> ion of the reference compound telocinobufagin,<sup>12</sup> suggesting that 5 could be telocinobufagin-3-*O*-sulfite. The LC-<sup>1</sup>H NMR spectra (S7 and S8) of 4 and 5 showed the ABX-type aromatic protons at  $\delta$  7.93 (1H, dd,  $J$  = 9.7, 2.6 Hz), 7.32 (1H, d,  $J$  = 2.6 Hz), and 6.11 ppm (1H, d,  $J$  = 9.7 Hz) for 4 and  $\delta$  7.87 (1H, dd,  $J$  = 9.8, 2.6 Hz), 7.30 (1H, d,  $J$  = 2.6 Hz), and 6.18 ppm (1H, d,  $J$  = 9.8 Hz) for 5. Two signals of methyl protons were observed at  $\delta$  0.72 (3H, s) and 0.92 ppm (3H, s) for 4 as well as  $\delta$  0.67 (3H, s) and 0.88 ppm (3H, s) for 5. The above-mentioned <sup>1</sup>H NMR data were identical with those of desacetylbufotalin and telocinobufagin.<sup>4,13</sup> Compounds 4 and 5 were thus identified as desacetylbufotalin-3-*O*-sulfite and telocinobufagin-3-*O*-sulfite.

Differing from compounds 1–5, compound 6 was deduced as a nonsulfated but acetylated bufadienolide on the basis of the MS<sup>n</sup> and NMR data. It showed  $\lambda_{\max}$  at 292 nm in the online UV spectrum, again indicating substitution close to the chromophore, and a molecular weight of 474 ( $m/z$  475 for the [M + H]<sup>+</sup> and  $m/z$  473 for the [M - H]<sup>-</sup>). The MS<sup>2</sup> spectrum (S9) of the [M + H]<sup>+</sup> ion of 6 clearly shows the neutral loss of acetic acid (60 Da) followed by the loss of up to three molecules of water. The reference compound arenobufagin<sup>14</sup> yielded the same type of ions in MS<sup>2</sup> (corresponding fragment ions are observed at +2 Da compared to 6), although the relative abundances are different. The <sup>1</sup>H NMR spectrum (S10) exhibited three aromatic signals of the  $\alpha$ -pyrone ring at  $\delta$  7.41 (1H, d,  $J$  = 2.6 Hz), 7.97 (1H, dd,  $J$  = 9.8, 2.6 Hz), and 6.14 ppm (1H, d,  $J$  = 9.8 Hz), two methyl signals at  $\delta$  0.96 (3H, s) and 1.15 ppm (3H, s), and an additional three-proton singlet at  $\delta$  1.83 ppm belonging to the acetyl group. Considering also the acetyl carbon signals at  $\delta$  171.8 and 20.9 ppm, compound 6 was deduced as a bufadienolide acetate. Compared to the <sup>13</sup>C NMR data of arenobufagin,<sup>15</sup> the resonances of C-15, C-16, and C-17 of 6 were observed to be shifted downfield to  $\delta$  40.6, 74.6, and 48.0 ppm, respectively (Table 3). Moreover, H-16 at  $\delta$  5.22 ppm showed correlations with H-17 at  $\delta$  4.38, H-15 $\alpha$  at 1.97, and H-15 $\beta$  at 1.84 ppm in the <sup>1</sup>H-<sup>1</sup>H COSY spectrum (S11). The above information revealed that the acetyl group was attached to C-16 of arenobufagin. In addition, the 2D COSY spectrum displayed correlations of H-3 with 3-OH at  $\delta$  2.43, the CH<sub>2</sub> protons in position 2 ( $\delta$  1.70 and 1.37 ppm) and 4 ( $\delta$  1.83 and 1.25 ppm), and correlations of H-11 with 11-OH at  $\delta$  3.72 (1H, d,  $J$  = 4.2 Hz) and H-9 at 1.75 ppm (1H, t,  $J$  = 11.5 Hz), which confirmed the positions of two hydroxy groups in the structure of 6. Signal assignments in Tables 2 and 3 were corroborated by HSQC and HMBC experiments. Thus, compound 6 is 16-*O*-acetylarenobufagin.



**Table 2.** <sup>1</sup>H NMR Data for Compounds **1**, **2**, **4**, **5**, and **6** (acetonitrile-*d*<sub>3</sub>, δ ppm, coupling constants in Hz)

	1	2	4	5	6
2a					1.70, m
2b					1.37, m
3	4.57, m	4.52, m	4.57, m	4.56, m	3.94, m
4a					1.83, m
4b					1.25, m
18	0.64, s	0.63, s	0.72, s	0.67, s	0.96, s
19	4.20, d (11.4) 3.36, d (11.4)	10.05, s	0.92, s	0.88, s	1.15, s
21	7.29, d (2.6)	7.29, d (2.6)	7.32, d (2.6)	7.30, d (2.6)	7.41, d (2.6)
22	7.86, dd (9.8, 2.6)	7.86, dd (9.8, 2.6)	7.93, dd (9.7, 2.6)	7.87, dd (9.8, 2.6)	7.97, dd (9.8, 2.6)
23	6.18, d (9.8)	6.18, d (9.8)	6.11, d (9.7)	6.18, d (9.8)	6.14, d (9.8)
11					4.39, dd (11.5, 4.2)
16			4.27, t (6.5)		5.22, ddd (8.5, 8.5, 1.5)
17					4.38, d (8.5)
COOCH <sub>3</sub>					1.83, s
11-OH					3.72, d (4.2)
3-OH					2.43, s
14-OH					3.33, d

**Table 3.** <sup>13</sup>C NMR Data for Compounds **1** and **6** (Methanol-*d*<sub>4</sub>, δ ppm)

no.	1	6	no.	1	6
1	20.2 CH <sub>2</sub>	33.0 CH <sub>2</sub>	14	86.1 C	85.7 C
2	25.8 CH <sub>2</sub>	29.3 CH <sub>2</sub>	15	32.9 CH <sub>2</sub>	40.6 CH <sub>2</sub>
3	77.1 CH	67.7 CH	16	29.7 CH <sub>2</sub>	74.6 CH
4	36.7 <sup>a</sup> CH <sub>2</sub>	34.6 CH <sub>2</sub>	17	52.1 CH	48.0 CH
5	77.0 C	39.4 CH	18	17.2 CH <sub>3</sub>	17.5 CH <sub>3</sub>
6	36.8 <sup>a</sup> CH <sub>2</sub>	27.8 CH <sub>2</sub>	19	65.3 CH <sub>2</sub>	23.9 CH <sub>3</sub>
7	25.2 CH <sub>2</sub>	22.7 CH <sub>2</sub>	20	125.0 C	117.9 C
8	41.8 CH	41.0 CH	21	150.5 CH	151.8 CH
9	40.1 CH	39.2 CH	22	149.3 CH	149.3 CH
10	43.8 C	38.2 C	23	115.4 CH	113.7 CH
11	22.9 CH <sub>2</sub>	74.9 CH	24	164.8 C=O	164.1 C=O
12	42.0 CH <sub>2</sub>	214.4 C=O		COCH <sub>3</sub>	171.8 C=O
13	49.5 C	64.7 C		COCH <sub>3</sub>	20.9 CH <sub>3</sub>

<sup>a</sup> Assignment interchangeable.

Bufadienolide sulfates were previously reported, either originating from the skin and bile of *B. vulgaris formaosus* Boulenger,<sup>16</sup> *B. marinus* Schneider,<sup>17,18</sup> and *B. bufo gargarizans* Cantor<sup>19</sup> or as in vitro metabolites of toad venom.<sup>20</sup> The present investigation represents the first finding of sulfate conjugates in *B. melanostictus*. Considering that the sulfated products are more water-soluble and more easily eliminated from the body<sup>21</sup> and, moreover, bufadienolide sulfates are less active than the potent bufotoxins and unconjugated bufadienolides,<sup>18,22</sup> the sulfation could be considered a detoxification pathway of bufadienolides from the animal body.

The in vitro growth inhibitory activity of compounds **1–6** and hellebrin (positive control) has been determined by means of the MTT colorimetric assay<sup>23,24</sup> in four human and two mouse cancer cell lines, whose histopathological characteristics are provided in Table 4. The data show that the in vitro cytotoxic activity of the six compounds varies on a >2 log-scale concentration when taking into account the human cancer cell lines, with compound **3** displaying cytotoxic activity similar to hellebrin (Table 4). The compounds displayed no cytotoxic activity in vitro up to 10 μM in the two mouse cancer cell lines (Table 4). Knowing that (i) cellular ligands of bufadienolides relate to the alpha subunits of the sodium pump (the Na<sup>+</sup>/K<sup>+</sup>-ATPase)<sup>25,26</sup> and (ii) the alpha-1 subunit of the sodium pump is twice mutated in rodent cells and about 1000-fold less sensitive to cardiotonic steroid effects than in human cells,<sup>25–28</sup> the data strongly suggest that the cytotoxic effects of the bufadienolides are mediated through the alpha-1 subunit of the sodium pump (Table 4). In addition, the current data also reveal large inter as well as intra (the large SD values in Table 4) human cancer cell line variations in terms of sensitivity to the compounds. This feature relates to the fact that the levels of alpha-1 subunit expression markedly vary in cancer cells, even in a given cancer.<sup>27–30</sup> In conclusion, compound **3** displays similar in vitro cytotoxic activity

when compared to hellebrin, and this activity seems mediated, at least partly, through the alpha-1 subunit of the sodium pump, i.e., the Na<sup>+</sup>/K<sup>+</sup>-ATPase.

### Experimental Section

**Materials and Reagents.** Toad venom, collected from the secretion of *B. melanostictus* Schneider in Indonesia, and the reference compounds hellebrigenol, 19-hydroxybufalin, desacetylbufotalin, telocinobufagin, and arenobufagin were kindly donated by Prof. Dr. Tadeus Reichstein (University of Basel, Switzerland). The purity of the reference compounds was >95% as determined by HPLC-UV analysis. MeCN (LiChrosolv, gradient-grade for LC, Merck, Darmstadt, Germany), ultrapure water (prepared in-house), and HOAc (Carl Roth, Karlsruhe, Germany) were used for LC analyses. The MeOH (VWR, Vienna, Austria) for sample preparation was p.a. grade.

**Preparative Isolation of Toad Venom Compounds.** The dried and powdered toad venom (4.0 g) derived from *B. melanostictus* was extracted three times for 1 h with MeOH under reflux. The combined extract was evaporated at 40 °C under reduced pressure to give 1.37 g of dry residue. For preparative HPLC fractionation, the residue was dissolved in MeOH to 150 mg/mL.

Preparative HPLC was performed on a Nucleosil C<sub>18</sub> column (21.0 × 250 mm, 10 μm, Macherey-Nagel, Düren, Germany) at a flow rate of 20 mL/min using a Shimadzu HPLC system (Shimadzu, Kyoto, Japan) equipped with an LC-8A solvent delivery pump and an SIL-10AP autosampler. Continuous monitoring of the effluent was achieved with an SPD-M20A diode array detector at 296 nm. The effluent was automatically collected by an FRC-10A collector (Shimadzu) in fractions corresponding to 0.5 min time intervals. Water (pH 3.3 with HOAc) and MeCN were used as mobile phase A and B, respectively. The following gradient program was used: 15% B (0 min), 28% B (30 min), 100% B (31 min), and 100% B (41 min). A typical HPLC profile of the toad venom MeOH extract is shown in Figure 2. The collected fractions from the preparative HPLC were analyzed on an analytical HPLC system using the same mobile phase and gradient program. The flow rate in this case was 0.8 mL/min. The fractions containing the same constituents were combined to give compound **1** (6.0 mg), Fr. II containing **1** and **2** (3.3 mg), Fr. III containing **3** (0.5 mg), Fr. IV containing **4** and **5** (6.4 mg), and Fr. V containing **6** (6.5 mg). The purity of compound **1** was determined by LC-UV analysis and off-line NMR. Fractions II–V were analyzed by LC-DAD-MS and LC-SPE-NMR.

**ESI-MS<sup>n</sup> Analysis of Reference Compounds.** All mass spectra were obtained on a 3D quadrupole ion trap instrument equipped with an orthogonal ESI source (HCT, Bruker Daltonics, Bremen, Germany). Reference compounds were dissolved to 0.2 mg/mL in MeOH and directly infused into the ESI source at a flow rate of 5 μL/min with a syringe pump (kdScientific, Holliston, MA). Source parameters were as follows: capillary voltage 4.0 kV, nebulizer 7 psi (N<sub>2</sub>), dry gas flow 4 L/min (N<sub>2</sub>), and dry temperature 250 °C. ESI-MS<sup>n</sup> spectra were recorded in positive ion mode under optimized conditions for ion transfer and fragmentation.

**HPLC/ESI-MS<sup>n</sup> Analysis of the Fractions II–V.** The LC-MS analyses were performed on an UltiMate 3000 RSLC-series system

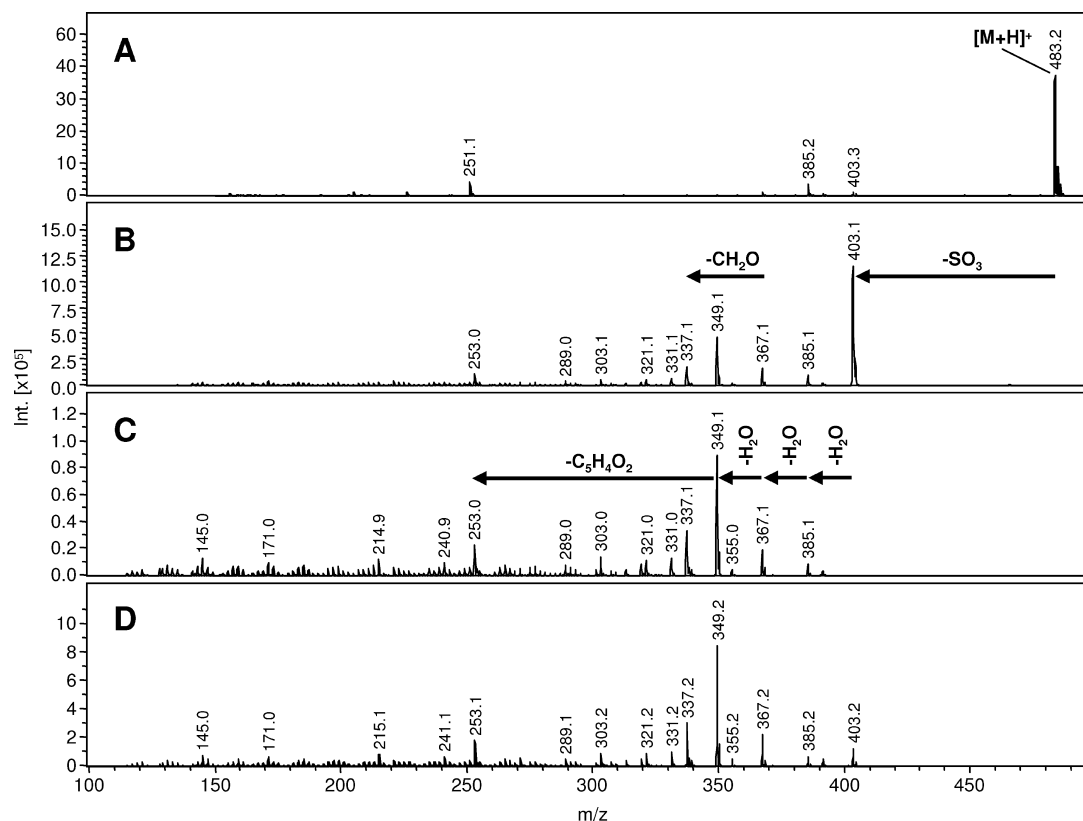


**Figure 4.** LC-ESIMS<sup>n</sup> analysis of compound **3** in fraction III: (A) MS spectrum showing the  $[M + H]^+$  ion at  $m/z$  483; (B) MS<sup>2</sup> spectrum of the  $[M + H]^+$  ion ( $m/z$  483  $\rightarrow$ ); (C) MS<sup>3</sup> spectrum of the  $[M - SO_3 + H]^+$  fragment ion ( $m/z$  483  $\rightarrow$  403  $\rightarrow$ ); (D) MS<sup>2</sup> spectrum of the  $[M + H]^+$  ion of the reference compound 19-hydroxybufalin ( $m/z$  403  $\rightarrow$ ).

**Table 4.** In Vitro Growth Inhibitory Activity Determination (MTT colorimetric assay)

compound	IC <sub>50</sub> growth inhibitory concentration (nM; mean $\pm$ SD)						
	human cancer cell lines				mean $\pm$ SEM	mouse cancer cell lines	
	A549 NSCLC	U373 GBM	Hs683 OLG	MCF-7 breast		B16F10 melanoma	CT26 colon
<b>1</b>	80 $\pm$ 4	323 $\pm$ 31	50 $\pm$ 7	120 $\pm$ 20	143	>10 000	>10 000
<b>2</b>	45 $\pm$ 16	396 $\pm$ 25	98 $\pm$ 33	507 $\pm$ 40	262	>10 000	>10 000
<b>3</b>	5 $\pm$ 1	12 $\pm$ 3	82 $\pm$ 29	150 $\pm$ 25	62	>10 000	>10 000
<b>4</b>	464 $\pm$ 45	525 $\pm$ 71	177 $\pm$ 11	3289 $\pm$ 349	1114	>10 000	>10 000
<b>5</b>	36 $\pm$ 14	51 $\pm$ 9	7 $\pm$ 1	1581 $\pm$ 669	419	>10 000	>10 000
<b>6</b>	1360 $\pm$ 531	878 $\pm$ 24	455 $\pm$ 12	2253 $\pm$ 801	1237	>10 000	>10 000
hellebrin	16 $\pm$ 5	49 $\pm$ 6	7 $\pm$ 1	82 $\pm$ 23	38	>10 000	>10 000

<sup>a</sup> The in vitro IC<sub>50</sub> growth inhibitory concentrations were determined by means of the MTT colorimetric assay. The cell lines include the human A549 non-small-cell lung cancer (NSCLC), the U373 glioblastoma (GBM), the Hs683 oligodendroglioma (OLG), and the MCF-7 breast cancer cell lines. The mouse cancer cell lines include the B16F10 melanoma and the CT26 colon cancer models.

(Dionex, Germering, Germany) coupled to the above-mentioned ESI ion trap mass spectrometer. HPLC separation was carried out on a Hypersil BDS-C<sub>18</sub> column (4.0  $\times$  250 mm, 5  $\mu$ m, Agilent, Germany) at a flow rate of 0.8 mL/min. Water (pH 3.3 with HOAc) and MeCN were used as mobile phase A and B, respectively. The following gradient program was used: 12% B (0 min), 32% B (40 min), 95% B (41 min), and 95% B (51 min). Fr. IV was alternatively analyzed on a Nucleosil C<sub>18</sub> column (4.0  $\times$  250 mm, 5  $\mu$ m, Macherey-Nagel) using identical mobile phases and flow rate but a shallower gradient: 24% B (0 min), 28% B (30 min), 100% B (31 min), and 100% B (41 min). The eluent flow was split roughly 1:8 before the ESI ion source, which was operated as follows: capillary voltage 4.0 kV, nebulizer 30 psi (N<sub>2</sub>), dry gas flow 7 L/min (N<sub>2</sub>), and dry temperature 350  $^{\circ}$ C. The mass spectrometer was operated in an automated data-dependent acquisition (DDA) mode where each MS scan ( $m/z$  150–900, average of 5 spectra) was followed by MS<sup>2</sup> scans ( $m/z$  40–900, average of 3 spectra, isolation window of 4 Th, fragmentation amplitude of 1.0 V) of the two most intense precursor ions and MS<sup>3</sup> scans ( $m/z$  40–900, average of 3 spectra, isolation window of 4 Th, fragmentation amplitude of 1.0 V) of the

most intense fragment ion in each MS<sup>2</sup> scan. In additional LC-MS experiments, the instrument was operated in alternating ion MS<sup>1</sup> mode.

**HPLC-SPE-NMR Analysis of the Fractions II–V.** LC-SPE-NMR analysis was performed on a Bruker BioSpin LC-SPE-NMR-600 system. Trapping was carried out using an Agilent 1200 liquid chromatograph, consisting of a HPLC quaternary pump, autosampler, Zorbax Eclipse XDB-C 18 column (4.6  $\times$  150 mm, 5  $\mu$ m), column oven (13  $^{\circ}$ C), and diode array detector. Mobile phase and flow rate were identical with those used for HPLC-MS analysis. The Bruker/Spark Prospect 2 solid-phase extraction unit was used to automatically trap the chromatographic peaks on HySphere Resin GP cartridges (10  $\times$  2 mm) after postcolumn addition of H<sub>2</sub>O (1.3 mL/min) using a Knauer K120 HPLC pump. Trapped peaks were first dried with nitrogen and eluted with acetonitrile-*d*<sub>3</sub> into an AVANCE 600 MHz spectrometer, equipped with an LC-SEI probe head with an active volume of 30  $\mu$ L (Bruker BioSpin).

**Offline NMR Analysis.** In addition to the above HPLC-SPE-NMR analysis, offline NMR spectra from compound **1** and part of the fractions were recorded on a Bruker Avance DRX 600 NMR spectrometer using

a 5 mm switchable quadruple probe (QNP,  $^1\text{H}$ ,  $^{13}\text{C}$ ,  $^{19}\text{F}$ ,  $^{31}\text{P}$ ) with  $z$  axis gradients and automatic tuning and matching accessory (Bruker BioSpin). The resonance frequency for  $^1\text{H}$  NMR was 600.13 MHz and for  $^{13}\text{C}$  NMR 150.92 MHz. All measurements were performed for a solution in methanol- $d_4$  at 298 K. Standard 1D and gradient-enhanced (ge) 2D experiments, such as DQFCOSY, TOCSY, NOESY, HSQC, and HMBC, were used as supplied by the manufacturer. Chemical shifts are referenced internally to the residual, nondeuterated solvent signal for  $^1\text{H}$  ( $\delta$  3.31 ppm) or to the carbon signal of the solvent for  $^{13}\text{C}$  ( $\delta$  49.00 ppm).  $^1\text{H}$  NMR data from the HPLC-SPE-NMR in acetonitrile- $d_3$  are also referenced internally to the residual, nondeuterated solvent signal ( $\delta$  1.94 ppm).

#### Determining $\text{IC}_{50}$ in Vitro Growth Inhibitory Concentrations.

The overall growth level of four human and two mouse cancer cell lines was determined using the colorimetric MTT [3-(4,5-dimethylthiazol-2-yl)diphenyl tetrazolium bromide, Sigma, Belgium] assay.<sup>19,20,23,25</sup> Briefly, the cell lines were incubated for 24 h in 96-microwell plates (at a concentration of 10 000 to 40 000 cells/mL culture medium depending on the cell type) to ensure adequate plating prior to cell growth determination. The assessment of cell population growth by means of the MTT colorimetric assay is based on the capability of living cells to reduce the yellow MTT [3-(4,5-dimethylthiazol-2-yl)-2,5-diphenyltetrazolium bromide] to the blue product formazan by a reduction reaction occurring in the mitochondria. The number of living cells after 72 h of culture in the presence (or absence: control) of the various compounds is directly proportional to the intensity of the blue color, which is quantitatively measured by spectrophotometry, in our case by a Biorad model 680XR (Biorad, Nazareth, Belgium) at a 570 nm wavelength (with a reference of 630 nm). Each experiment was carried out in sextuplicate.

The four human cancer cell lines include the A549 non-small-cell lung cancer, the U373 glioblastoma, the Hs683 oligodendroglioma, and the MCF-7 breast cancer cell lines. The two mouse cancer cell lines used were the B16F10 melanoma and the CT26 colon cancer cell lines. The origin and cell culture conditions for each cell line are as follows. The human cell lines include the A549 (DSMZ (Deutsche Sammlung von Mikroorganismen und Zellkulturen; Braunschweig, Germany) code ACC107) non-small-cell lung cancer (NSCLC), the U373 (ECACC (European Collection of Cell Culture; Salisbury, UK) code 89081403) glioblastoma (GBM), the Hs683 (ATCC (American Type Culture Collection, Manassas, VA) code HTB-138) oligodendroglioma, and the MCF-7 (DSMZ code ACC115) breast cancer cell lines. The mouse cancer cell lines include the B16F10 (ATCC code CRL-6475) melanoma and CT26 (ATCC code CRL-2638) colon cancer cell lines. The cells were cultured in RPMI (Invitrogen, Merelbeke, Belgium) media supplemented with 10% heat-inactivated fetal calf serum (Invitrogen). All culture media were supplemented with 4 mM glutamine, 100  $\mu\text{g}/\text{mL}$  gentamicin, and penicillin-streptomycin (200 U/mL and 200  $\mu\text{g}/\text{mL}$ ) (Invitrogen).

**Acknowledgment.** This research work is part of the project "Quality Assurance of Herbal Medicinal Products (HMPs) from TCM", aided by the Austrian Federal Ministry of Science and Research and the Federal Ministry for Health, Family and Youth and was also supported by the National Natural Science Foundation of China (Grant No. 30801512). The first author is thankful to Eurasia Pacific Uninet for providing a postdoc scholarship. L.M.Y.B. is a research assistant and R.K. a director of research with the Fonds National de la Recherche Scientifique (FNRS, Belgium).

**Supporting Information Available:** LC-MS and NMR data for compounds 1–6. This material is available free of charge via the Internet at <http://pubs.acs.org>.

#### References and Notes

- (1) Committee for the Pharmacopoeia of P.R. China. *Pharmacopoeia of the People's Republic of China 2005 (English ed.)*; Chemical Industry Press: Beijing, China, 2005; Part I, p 265.
- (2) Verpoorte, R.; Kinh, P. Q.; Svendsen, A. B. *J. Ethnopharmacol.* **1979**, *1*, 197–202.
- (3) Iseli, E.; Weiss, E.; Reichstein, T.; Chen, K. K. *Helv. Chim. Acta* **1964**, *47*, 116–119.
- (4) Verpoorte, R.; Kinh, P. Q.; Svendsen, A. B. *J. Nat. Prod.* **1980**, *43*, 347–352.
- (5) Shimada, K.; Ohishi, K.; Nambara, T. *Chem. Pharm. Bull.* **1984**, *32*, 4396–4401.
- (6) Meng, Z.; Yang, P.; Shen, Y.; Bei, W.; Zhang, Y.; Ge, Y.; Newman, R. A.; Cohen, L.; Liu, L.; Thornton, B.; Chang, D. Z.; Liao, Z.; Kurzrock, R. *Cancer* **2009**, *115*, 5309–5318.
- (7) Garg, A. D.; Kanitkar, D. V.; Hippargi, R. V.; Gandhare, A. N. *Nature Precedings*. doi:10.1038/npre.2007.1204.1. Posted Oct 3, 2007.
- (8) Das, M.; Mallick, B. N.; Dasgupta, S. C.; Gomes, A. *Toxicol.* **2000**, *38*, 1267–1281.
- (9) Dasgupta, A. *Am. J. Clin. Pathol.* **2003**, *120*, 127–137.
- (10) Ye, M.; Guo, D. A. *Rapid Commun. Mass Spectrom.* **2005**, *19*, 1881–1892.
- (11) Tempone, A. G.; Pimenta, D. C.; Lebrun, I.; Sartorelli, P.; Taniwaki, N. N.; de Andrade, H. F.; Antoniazzi, M. M.; Jared, C. *Toxicol.* **2008**, *52*, 13–21.
- (12) Meyer, K. *Helv. Chim. Acta* **1949**, *32*, 1593–1599.
- (13) Reynolds, W. F.; Maxwell, A.; Telang, B.; Bedaisie, K.; Ramcharan, G. *Magn. Reson. Chem.* **1995**, *33*, 412–414.
- (14) Hofer, P.; Linde, H.; Meyer, K. *Tetrahedron Lett.* **1959**, *7*, 8–11.
- (15) Robien, W.; Kopp, B.; Schabl, D.; Schwarz, H. *Prog. Nucl. Magn. Reson. Spectrosc.* **1987**, *19*, 131–181.
- (16) Shimada, K.; Fujii, Y.; Nambara, T. *Tetrahedron Lett.* **1974**, *32*, 2767–2768.
- (17) Shimada, K.; Nambara, T. *Chem. Pharm. Bull.* **1979**, *27*, 1881–1886.
- (18) Lee, S. S.; Derguini, F.; Bruening, R. C.; Nakanishi, K.; Wallick, E. T.; Akizawa, T.; Rosenbaum, C. S.; Butler, V. P. *Heterocycles* **1994**, *39*, 669–686.
- (19) Shimada, K.; Ro, J. S.; Kanno, C.; Nambara, T. *Chem. Pharm. Bull.* **1987**, *35*, 4996–4999.
- (20) Shimada, K.; Miyashiro, Y.; Nishio, T. *Biomed. Chromatogr.* **2006**, *20*, 1321–1327.
- (21) Yi, L.; Dratter, J.; Wang, C.; Tunge, J. A.; Desaire, H. *Anal. Bioanal. Chem.* **2006**, *386*, 666–674.
- (22) Butler, V. P.; Morris, J. F.; Akizawa, T.; Matsukawa, M.; Keating, P.; Hardart, A.; Furman, I. *Am. J. Physiol. Regul. Integr. Comp. Physiol.* **1996**, *271*, R325–R332.
- (23) Van Quaquebeke, E.; Simon, G.; André, A.; Dewelle, J.; El Yazidi, M.; Bruyneel, F.; Tuti, J.; Nacoulma, O.; Guissou, P.; Decaestecker, C.; Braekman, J. C.; Kiss, R.; Darro, F. *J. Med. Chem.* **2005**, *48*, 849–856.
- (24) Lamoral-Theys, D.; Andolfi, A.; Van Goietsenoven, G.; Cimmino, A.; Le Calvé, B.; Wauthoz, N.; Mégazzini, V.; Gras, T.; Bruyère, C.; Dubois, J.; Mathieu, V.; Kornienko, A.; Kiss, R.; Evidente, A. *J. Med. Chem.* **2009**, *52*, 6244–6256.
- (25) Mijatovic, T.; Van Quaquebeke, E.; Delest, B.; Debeir, O.; Darro, F.; Kiss, R. *Biochim. Biophys. Acta* **2007**, *1776*, 32–57.
- (26) Mijatovic, T.; Ingrassia, L.; Facchini, V.; Kiss, R. *Expert Opin. Ther. Targets* **2008**, *12*, 1403–1417.
- (27) Mijatovic, T.; Roland, I.; Van Quaquebeke, E.; Nilson, B.; Mathieu, A.; Van Vynckt, F.; Darro, F.; Blanco, G.; Facchini, V.; Kiss, R. *J. Pathol.* **2007**, *212*, 170–179.
- (28) Mijatovic, T.; De Nève, N.; Gailly, P.; Mathieu, V.; Haibe-Kains, B.; Bontempi, G.; Lapeira, J.; Decaestecker, C.; Facchini, V.; Kiss, R. *Mol. Cancer Ther.* **2008**, *7*, 1285–1296.
- (29) Lefranc, F.; Mijatovic, T.; Kondo, Y.; Sauvage, S.; Roland, I.; Debeir, O.; Krstic, D.; Vasic, V.; Gailly, P.; Kondo, S.; Blanco, G.; Kiss, R. *Neurosurgery* **2008**, *62*, 211–221.
- (30) Mathieu, V.; Pirker, C.; de Lassalle, E. M.; Vernier, M.; Mijatovic, T.; De Nève, N.; Gaussin, J. F.; Dehoux, M.; Lefranc, F.; Berger, W.; Kiss, R. *J. Cell Mol. Med.* **2009**, *13*, 3960–3972.

NP900746K